Polarization and Electroweak Precision Measurements at the ILC for $\sqrt{s} = 250\,\mathrm{GeV}$

DPG-Frühjahrstagung, Würzburg

Robert Karl[1,2]

[1] DESY

[2] Universität Hamburg

22.03.2018

Universität Hamburg
DER FORSCHUNG | DER LEHRE | DER BILDUNG

DESY

HELMHOLTZ
RESEARCH FOR GRAND CHALLENGES

PIER

PIER Helmholtz Graduate School
A Graduate Education Program of Universität Hamburg in Cooperation with DESY

Collaborative Research Centre 676
Particles, Strings, and the Early Universe
The Structure of Matter and Space-Time

The International Linear Collider (ILC)

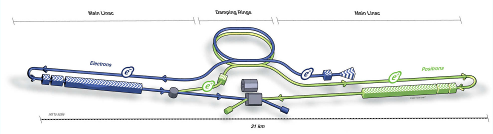

- Future linear e^+e^- collider:
  $\sqrt{s} = 250\,\text{GeV}$ (As a first stage)
- Construction under political consideration
  in the Kitakami region, Prefecture Iwate, Japan
- **At the ILC both beams (e^+, e^-) are polarized:** $P_{e^-} = \pm 80\%, \quad P_{e^+} = \pm 30\%$
- **Switch of polarization sign (helicity reversal) $\rightarrow$ choice of spin configuration**
- Designed for precision studies for physics of the standard model and beyond

Anomalous Triple Gauge Couplings (aTGCs)

TGC for e.g.:
single W

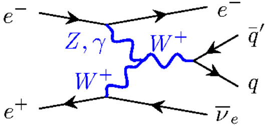

and W-pair production

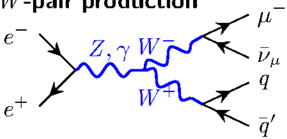

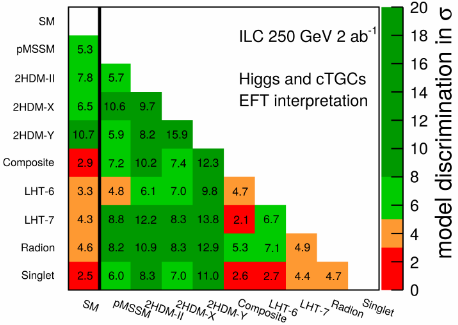

arXiv:1708.08912v1 [hep-ph]

- The constraint of TGCs and their precision of $\approx 10^{-3}$ is necessary for the distinction of different Higgs-models beyond the SM
- Additional bosons (e.g. Z') will affect TGCs

⇒ TGCs have to be precisely measured

⇒ aTGCs described by an Effective Field Theory (EFT)

ILC Aims for Precision Measurements

Triple Gauge Couplings (TGC)

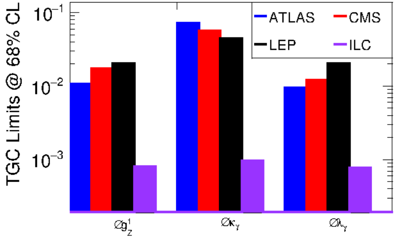

8 TeV ATLAS: $20.3\ \mathrm{fb}^{-1}$; CMS: $19.4\ \mathrm{fb}^{-1}$

⇒ **Polarization has to be known as precisely as the luminosity!**

⇒ **Requirement for a permille-level precision of the luminosity-weighed average polarization**

Previously achieved polarization precision

HERA: $\Delta P/P = 2\%_{\text{stat}} \oplus 1\%_{\text{sys}}$ [1] SLAC: $\Delta P/P = 1.1\%$ [2]

⇒ **More than one order of magnitude better precision on both TGC and polarization measurement** (for $2\,\mathrm{ab}^{-2}$ at 250 GeV)

⇒ **Accomplished by simultaneous measurement of both of them**

Beam Polarization Dependent Cross Section

- Theoretical polarized cross section in general:

$$\sigma_{\text{theory}}(P_{e^-}, P_{e^+}) = \frac{(1-P_{e^-})}{2}\frac{(1-P_{e^+})}{2}\cdot\sigma_{\text{LL}} + \frac{(1+P_{e^-})}{2}\frac{(1+P_{e^+})}{2}\cdot\sigma_{\text{RR}} + \frac{(1-P_{e^-})}{2}\frac{(1+P_{e^+})}{2}\cdot\sigma_{\text{LR}} + \frac{(1+P_{e^-})}{2}\frac{(1-P_{e^+})}{2}\cdot\sigma_{\text{RL}}$$

- Nominal ILC polarization values

$$\underbrace{P^-_{e^-} = -80\%,}_{\text{"left"-handed } e^- \text{-beam}} \quad \underbrace{P^+_{e^-} = 80\%,}_{\text{"right"-handed } e^- \text{-beam}} \quad \underbrace{P^-_{e^+} = -30\%,}_{\text{"left"-handed } e^+ \text{-beam}} \quad \underbrace{P^+_{e^+} = 30\%,}_{\text{"right"-handed } e^+ \text{-beam}}$$

- Cross section of the 4 polarization configurations

$$\sigma_{--} := \sigma\left(P^-_{e^-}, P^-_{e^+}\right) \qquad \sigma_{++} := \sigma\left(P^+_{e^-}, P^+_{e^+}\right)$$

$$\sigma_{-+} := \sigma\left(P^-_{e^-}, P^+_{e^+}\right) \qquad \sigma_{+-} := \sigma\left(P^+_{e^-}, P^-_{e^+}\right)$$

- σ_{LL}, σ_{RR}, σ_{LR}, σ_{RL} are theoretically calculated including Initial State Radiation (ISR) and beam spectrum

Polarized Cross Section Measurement

- Measured polarized cross section:

$$\sigma_{\text{data}} = \frac{D - \mathfrak{B}}{\varepsilon \cdot \mathcal{L}}$$

D:	Number of selected events	$\mathfrak{B}$:	Background expectation value
ε:	Detector selection efficiency	$\mathcal{L}$:	Integrated luminosity

Remark:

All of them can variate between the different data sets $(\sigma_{-+},\ \sigma_{+-},\ \sigma_{--},\ \sigma_{++})$

- Uncertainty of the polarized cross section is calculated via error propagation

Remark:

Statistical uncertainty is always uncorrelated: $\text{corr}\left(\sigma_i^D,\ \sigma_j^D\right) \equiv \delta_{ij}$

And it is determined by Poisson fluctuations: $\Delta D \equiv \sqrt{D}$

Usage of the Differential Polarized Cross Section

e.g.: $e^+e^- \rightarrow W^+W^- \rightarrow q\bar{q}'\mu^-\bar{\nu}$

Choice of the angle:

- ✓ Individual for each channel
- ✓ High dependence of the angular distribution on the chiral structure
- ✓ Angle has to be well measurable
- ✓ Multi-angle distribution available

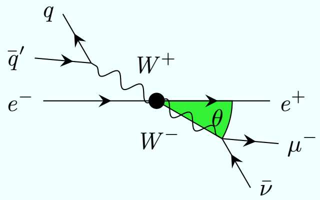

Projection on the θ_{W^-}-axis

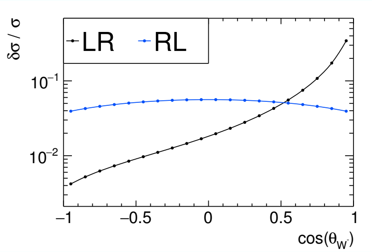

Bin-wise cross section calculation:

- Cross section calculated for each bin:
  - → Labeled for the i-th bin as $\delta_i\sigma$
- Analog for the selected events, background and selection efficiency
  - → Calculated bin-wise

Effect of Anomalous TGC in $e^- e^+ \to \mu\nu q\bar{q}$ at 250 GeV

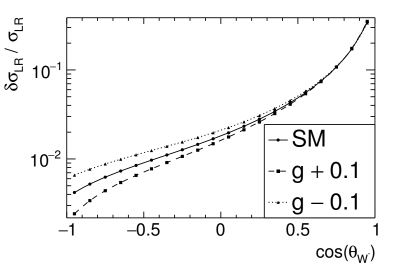

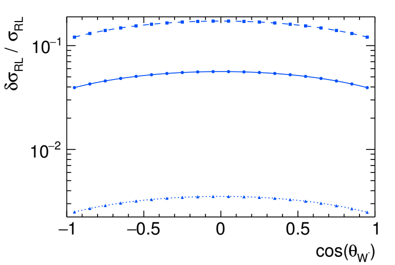

- The effect of the TGC g on the angular distribution
  - Variation the TGC within $\pm 10\%$ corresponds to $\pm 5\sigma$ deviation at LEP

  $\Rightarrow$ Only a very small impact on the angular distribution

  $\Rightarrow$ Especial sensitive only for ranges of low differential cross sections

- Precision measurement of TGCs:
  - A clear angular dependence: Event rates are affected simultaneously over the full angular range

  $+$ Strong dependence of the chiral structure

Fit Procedure

- **Considered Channels and their Parameters:**

channel	cross section	left-right asymmetry	TGC
$e^- e^+ \longrightarrow e^- \bar{\nu} q\bar{q}$	$\sigma_{e^-\bar{\nu}q\bar{q}}$	$A_{RR}^{e^-\bar{\nu}q\bar{q}} = \frac{\sigma_{LR}-\sigma_{RR}}{\sigma_{LR}+\sigma_{RR}}$	$g_Z^1,\ \kappa_\gamma,\ \lambda_\gamma$
$e^- e^+ \longrightarrow e^+ \nu q\bar{q}$	$\sigma_{e^+\nu q\bar{q}}$	$A_{LL}^{e^+\nu q\bar{q}} = \frac{\sigma_{LR}-\sigma_{LL}}{\sigma_{LR}+\sigma_{LL}}$	$g_Z^1,\ \kappa_\gamma,\ \lambda_\gamma$
$e^- e^+ \longrightarrow \mu\nu q\bar{q}$	$\sigma_{\mu\nu q\bar{q}}$	$A_{RL}^{\mu\nu q\bar{q}} = \frac{\sigma_{LR}-\sigma_{RL}}{\sigma_{LR}+\sigma_{RL}}$	$g_Z^1,\ \kappa_\gamma,\ \lambda_\gamma$
$e^- e^+ \longrightarrow \mu^+\mu^- q\bar{q}$	$\sigma_{\mu\mu q\bar{q}}$	$A_{RL}^{\mu\mu q\bar{q}} = \frac{\sigma_{LR}-\sigma_{RL}}{\sigma_{LR}+\sigma_{RL}}$	–
$e^- e^+ \longrightarrow q\bar{q}$	$\sigma_{q\bar{q}}$	$A_{RL}^{q\bar{q}} = \frac{\sigma_{LR}-\sigma_{RL}}{\sigma_{LR}+\sigma_{RL}}$	–
$e^- e^+ \longrightarrow ll$	σ_{ll}	$A_{RL}^{ll} = \frac{\sigma_{LR}-\sigma_{RL}}{\sigma_{LR}+\sigma_{RL}}$	–

- $P_{e^-}^-,\ P_{e^-}^+,\ P_{e^+}^-,\ P_{e^+}^+$ **determined globally for all channels**
- **Using the method of least squares:**

$$\chi^2 = \sum_{\text{channel}} \left[\sum_{\text{bin } i} \left(\delta_i\vec{\sigma}_{\text{data}} - \delta_i\vec{\sigma}_{\text{theory}}\right)^T \left(\delta_i\Xi\right)^{-1} \left(\delta_i\vec{\sigma}_{\text{data}} - \delta_i\vec{\sigma}_{\text{theory}}\right) \right];$$

$$\vec{\sigma} := \begin{pmatrix} \delta_i\sigma_{-+} & \delta_i\sigma_{+-} & \delta_i\sigma_{--} & \delta_i\sigma_{++} \end{pmatrix}^T$$

Results

Using the following global parameter values:

$$\varepsilon = 0.6$$

$$\pi = \frac{D - \mathfrak{B}}{D} = 0.8$$

$$\mathcal{L} = 2\,\mathrm{ab}^{-1}$$

$$\Delta\varepsilon = \Delta\pi = \Delta\mathcal{L} = 0$$

Luminosity sharing:

$$-+: 45\%, \quad +-: 45\%,$$
$$--: 5\%, \quad ++: 5\%$$

All results are in the order of 10^{-3}!

Cross Section $[10^{-4}]$

$\Delta\sigma_{e^+\nu q\bar{q}}/\sigma$	12.9
$\Delta\sigma_{e^-\bar{\nu} q\bar{q}}/\sigma$	13.3
$\Delta\sigma_{\mu\nu q\bar{q}}/\sigma$	11.4
$\Delta\sigma_{\mu\mu q\bar{q}}/\sigma$	13.8
$\Delta\sigma_{q\bar{q}}/\sigma$	3.78
$\Delta\sigma_{ll}/\sigma$	3.91

Asymmetry $[10^{-4}]$

$\Delta A_{RR}^{e^+\nu q\bar{q}}$	6.37
$\Delta A_{LL}^{e^-\bar{\nu} q\bar{q}}$	19.1
$\Delta A_{LR}^{\mu\nu q\bar{q}}$	3.32
$\Delta A_{LR}^{\mu\mu q\bar{q}}$	15.4
$\Delta A_{LR}^{q\bar{q}}$	6.66
ΔA_{LR}^{ll}	7.72

Polarization $[10^{-4}]$

$\Delta P_{e^-}^-$	7.68
$\Delta P_{e^-}^+$	3.4
$\Delta P_{e^+}^-$	8.11
$\Delta P_{e^+}^+$	10.7

TGC $[10^{-4}]$

Δg	8.18
$\Delta\kappa$	10.1
$\Delta\lambda$	9.33

Conclusion

- **Polarization provides a deep insight into the chiral structure of the standard model and beyond**
  - A permille-level precision of the luminosity-weighted average polarization at the IP is required
- **A full electroweak precision fit is achievable at the ILC**
  - The beam polarization, unpolarized cross section, the left-right asymmetry and anomalous Triple Gauge couplings can be determined with a relative precision of $\mathcal{O}\left(10^{-3}\right)$
- **Additional studies on the dependence of systematic quantities and their uncertainties will follow**

References

[1] S. Baudrand, M Bouchela, V Brissona, R Chichea, M Jacqueta, S Kurbasova, G Lia, C Pascauda, A Rebouxa, V Soskova, Z Zhanga, F Zomera, M Beckinghamb, T Behnkeb, N Coppolab, N Meynersb, D Pitzlb, S Schmittb, M Authierc, P Deck-Betinellic, Y Queinecc and L Pinardd, *A high precision Fabry-Perot cavity polarimeter at HERA*, Journal of Instrumentation 2010, (http://www.slac.stanford.edu/cgi-wrap/getdoc/slac-pub-6700.pdf)

[2] P. C. ROWSON, *PRECISION ELECTROWEAK PHYSICS WITH THE SLD/SLC: THE LEFT-RIGHT POLARIZATION ASYMMETRY*, SLAC-PUB-6700, December 1994, (http://www.slac.stanford.edu/cgi-wrap/getdoc/slac-pub-6700.pdf)

Backup Slides

Polarized Cross Section Measurement

- Measured polarized cross section:

$$\sigma_{\text{data}} = \frac{D - \mathfrak{B}}{\varepsilon \cdot \mathcal{L}}$$

D:	Number of selected events	$\mathfrak{B}$:	Background expectation value
ε:	Detector selection efficiency	$\mathcal{L}$:	Integrated luminosity

Remark:
All of them can variate between the different data sets $(\sigma_{-+},\ \sigma_{+-},\ \sigma_{--},\ \sigma_{++})$

- Uncertainty of the polarized cross section is calculated via error propagation

$$\text{e.g.}\quad (\Xi_{\mathcal{L}})_{ij} = \text{corr}\left(\sigma_i^{\mathcal{L}},\ \sigma_j^{\mathcal{L}}\right) \frac{\partial \sigma_i}{\partial \mathcal{L}_i} \frac{\partial \sigma_j}{\partial \mathcal{L}_j} \Delta\mathcal{L}_i \Delta\mathcal{L}_j \qquad i,j \in \{-+, +-, --, ++\}$$

$$\Xi := \underbrace{\Xi_D}_{\substack{\text{statistical}\\ \text{uncertainty}}} + \underbrace{\Xi_{\mathfrak{B}} + \Xi_{\varepsilon} + \Xi_{\mathcal{L}}}_{\text{systematic uncertainty}};$$

Remark:
Statistical uncertainty is always uncorrelated: $\text{corr}\left(\sigma_i^D,\ \sigma_j^D\right) \equiv \delta_{ij}$
And it is determined by Poisson fluctuations:
$\Delta D \equiv \sqrt{D}$

TGC Contribution for the Final State

$e^+e^- \to e\nu q\bar{q}$

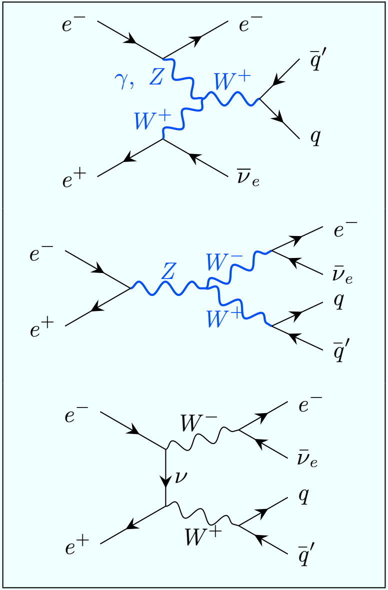

$e^+e^- \to \mu\nu q\bar{q}$

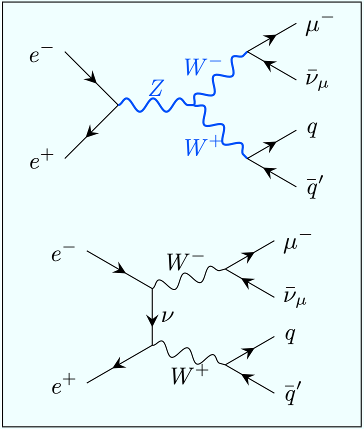

ILC Polarimetry Concept for Permille-Level Polarization Precision

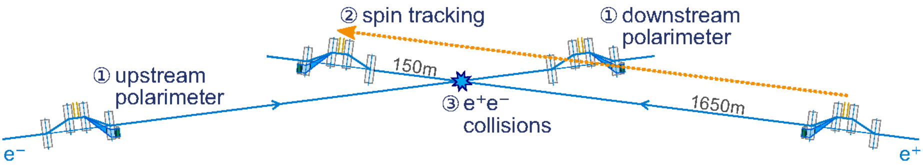

- **The time-resolved beam polarization:**
  - Measured with 2 laser-Compton polarimeters before and after the $e^- e^+$ IP
  - Polarimeter precision $\Delta P/P = 0.25\%$ from the start
  - Extrapolated to the $e^- e^+$ IP via spin tracking

\+ **The luminosity-weighed averaged polarization:**

  - Calculated from collision data at the IP
  - Using the cross section measurement of well known standard model processes

⇒ **Combination of both measurements**

→ With the aim to reach the permille-level precision $\Delta P/P = 0.1\%$

Testing for a Non-Perfect Helicity Reversal

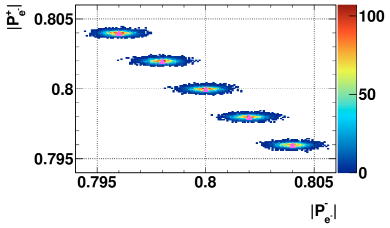

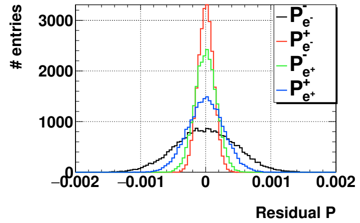

- **Variation in the absolute polarization**
  - Toy Measurement for 5 different polarization discrepancies for both beams
  - Nominal initial polarizations: $|P_{e-}| = 80\%$, $|P_{e+}| = 30\%$
  - Statistical uncertainties only
- χ^2**-Fit:**
  - Correct determination of the 4 polarization values
  - No noticeable impact on polarization precision using total cross sections

✓ **Can compensate for a non-perfect helicity reversal**

Consider Constraints from the Polarimeter Measurement

Simplified approach:
(as a first step)

- Neglect spin transport
- Using $\Delta P/P = 0.25\%$:
- Gaussian distribution
  - Mean: $|P_{e^-}| = 80\%, |P_{e^+}| = 30\%$
  - Width: ΔP

Implementation:

$$\chi'^2 = \chi^2 + \sum_P \left[\frac{\left(P^{\pm}_{e^{\pm}} - \mathcal{P}^{\pm}_{e^{\pm}}\right)^2}{\Delta\mathcal{P}^2} \right]$$

- $P^{\pm}_{e^{\pm}}$: 4 fitted parameters
- $\mathcal{P}^{\pm}_{e^{\pm}}$: Polarimeter measurement
- $\Delta\mathcal{P}$: Polarimeter uncertainty

E[GeV]	**500**	**350**	**250**	**500**	**250**
$\mathcal{L}$[1/fb]	**500**	**200**	**500**	**3500**	**1500**
$\left[10^{-3}\right]$	**Without Constraint**				
$\Delta P^-_{e^-}/P$	1.9	2.8	1.4	0.74	0.84
$\left[10^{-3}\right]$	**With Constraint**				
$\Delta P^-_{e^-}/P$	1.1	1.2	0.93	0.63	0.69

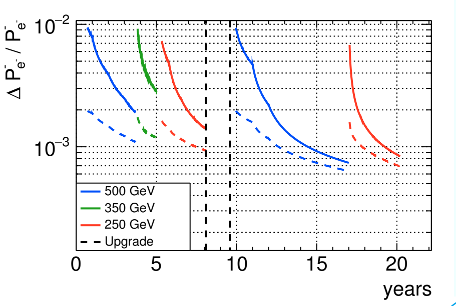

Polarization at an $e^- e^+$ Collider

- **Consider only one electron positron pair:**
  - Helicity is the projection of the spin vector on the direction of motion
  - In case of massless particles, helicity is equal to chirality (left and right handedness)
  - If $E_{\text{kin}} \gg E_0 \quad \longrightarrow \quad m_e \approx 0$ e.g. ILC: $E_{\text{kin}}/E_0 \approx \mathcal{O}\left(10^5 - 10^6\right)$

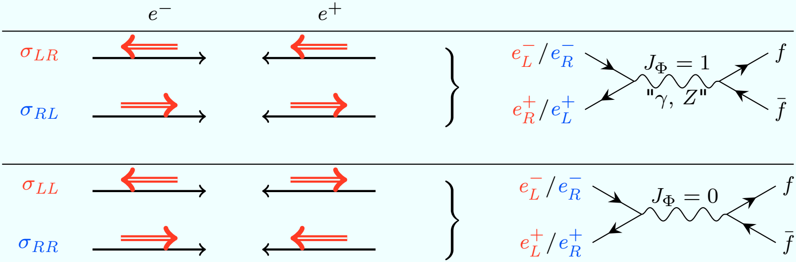

- **For a bunch of particles the polarization P is defined as:**

$$P := \frac{N_R - N_L}{N_R + N_L} \qquad \begin{cases} N_R : & \text{The number of right-handed particles} \\ N_L : & \text{The number of left-handed particles} \end{cases}$$

Production of Polarized Beams

Electron beam:

- Shooting of a circular polarized laser on a photocathode
- Switch between polarization signs (helicity reversal)
  - $\Rightarrow$ Switch between signs of the laser polarization

Positron beam:

- Production of circular polarized γ's from e^--beam propagating through a helical undulator
  - $\Rightarrow$ e^+ obtained via pair-production of the γ's
- Helicity reversal
  - $\Rightarrow$ Switch between two beam lines

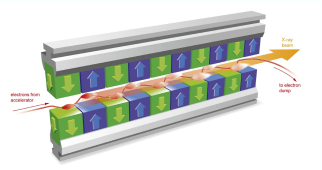

www.xfel.eu/ueberblick/funktionsweise/

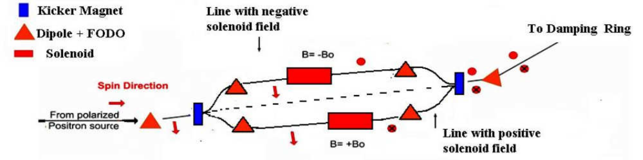

Laser-Compton Polarimeters

Magnetic chicane of the upstream polarimeters

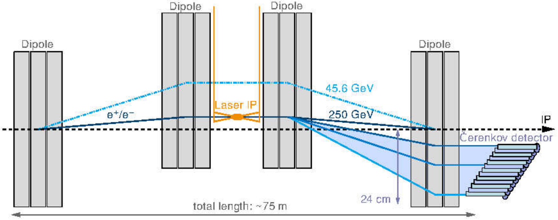

- Compton scattering of the beam with a polarized Laser
- $\mathcal{O}(10^3)$ particles per bunch $(2 \cdot 10^{10})$ are scattered
- Magnetic chicane: energy spectrum $\Rightarrow$ spatial distribution

- Energy spectrum measurement:
  $\Rightarrow$ Counting the scattered particles at different positions
- Design of the magnetic Chicane:
  - Laser-bunch interaction point moves with beam energy
    $\longrightarrow$ position of the Compton edge stays the same
  - Orbit of the non-scattered particles is unaffected by the magnetic chicane

Downstream Polarimeter

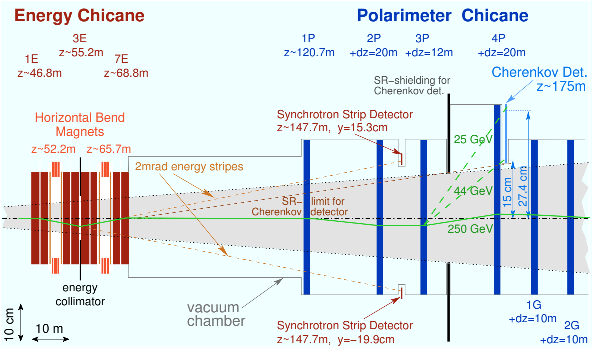

Difference to Upstream Polarimeter due to a large disturbed beam

- Stronger banding of the beam after γ-IP
- 2 additional magnets to restore the beam orbit
- Measuring one bunch per train

Cherenkov Detectors: Basic Concept

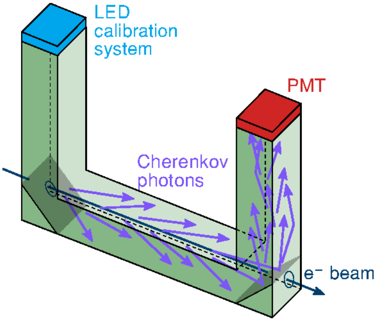

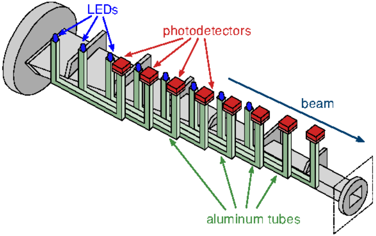

- U-shape channels filled with gas: e.g. perfluorobutane
- Concept
  - Scattered particles propagates through the bottom
  - Produced Cherenkov light is reflected to one end of the channel
  - Light measurement with photomultiplier tube (PMT)
- At the other end: LED for PMT calibration
- Sampling of the energy distribution → Number of Cherenkov detector
- Energy resolution → Thickness of a Cherenkov detector
- Quartz Cherenkov detector concept: Ref.: Theses Annika Vauth

http://bib-pubdb1.desy.de/record/171400

Differential Compton Cross Section

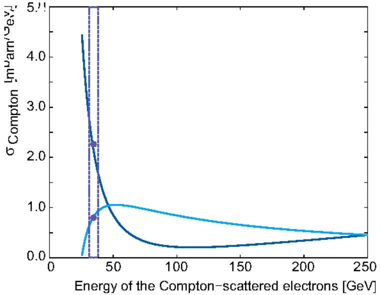

Energy dependence:

$$\frac{\mathrm{d}\sigma_C}{\mathrm{d}y_C} = \frac{2\pi r_e^2}{x_C}\left(a_C + \lambda\mathcal{P}\cdot b_C\right); \quad y_C := 1 - \frac{E'}{E}$$

e^- Polarization: $\mathcal{P}$; Laser Polarization: λ

DarkBlue: $\lambda\mathcal{P} = +1$

Cyan: $\lambda\mathcal{P} = -1$

Calculating $\mathcal{P}_i$ of the i-th channel with asymmetry A_i, analysing power Π_i

$$A_i := \frac{N_i^- - N_i^+}{N_i^- + N_i^+}; \qquad \Pi_i = \frac{\mathcal{I}_i^- - \mathcal{I}_i^+}{\mathcal{I}_i^- + \mathcal{I}_i^+}; \qquad \mathcal{I}_i^{\pm} := \int_{E_i-\Delta/2}^{E_i+\Delta/2} \left.\frac{\mathrm{d}\sigma_C}{\mathrm{d}y_C}\right|_{\lambda\mathcal{P}=\pm1} \mathrm{d}y_C$$

$N^{\pm} := \#e_{\text{Compton}}$ for $\lambda\mathcal{P} = \pm1$; E_i : energy of i-th channel; Δ : energy width

$$\Rightarrow \quad \lambda\mathcal{P}_i = \frac{A_i}{\Pi_i} \quad \Rightarrow \quad \mathcal{P} = \langle\mathcal{P}_i\rangle$$

Compton Scattering Cross Section: Formulary

$$\frac{d\sigma}{dy_C} = \frac{2\pi r_e^2}{x_C}\left(a_C + \lambda\mathcal{P}\cdot b_C\right)$$

$$y_C := 1 - \frac{E'_\gamma}{E}; \quad x_C := \frac{4EE_\gamma}{m_e^2}\cos^2\left(\frac{\vartheta_0}{2}\right)$$

$$r_C := \frac{y_C}{x_C\left(1-y_C\right)}$$

$$a_C := \left(1-y_C\right)^{-1} + 1 - y_C - 4r_C\left(1-r_C\right)$$

$$b_C := r_C x_C\left(1-2r_C\right)\left(2-y_C\right)$$

$E,\ E_\gamma$:	e^-,γ energy before Compton scattering
$E',\ E'_\gamma$:	e^-,γ energy after Compton scattering
$m_e,\ r_e$:	mass, classical radius of e^-
ϑ_0 :	crossing angle between e^-,γ
$\mathcal{P}$:	longitudinal polarization of e^-
λ :	circular polarization of γ_{Laser}

Characteristic Point:

$$E'_{\text{crossover}} = \frac{E}{1+x_C/2}, \qquad E'_{\text{ComptonEdge}} = E'_{\text{min}} = \frac{E}{1+x_C}$$

Spin Precession

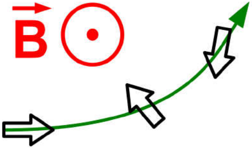

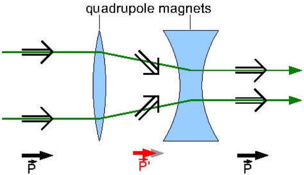

- Polarimeters are 1.65 km and 150 m away from IP
  - → Particles propagate through magnets
  - → Magnets influence the spin, as well
  - → Described by Thomas precession
- if $\vec{B}_{\parallel} = \vec{E} = 0$:

$$\frac{\mathrm{d}}{\mathrm{d}t}\vec{S} = -\frac{q}{m\gamma}\left((1+a\gamma)\,\vec{B}_{\perp}\right) \times \vec{S}$$

- Effects from focusing and defocusing can cancel
- For a series of quadrupole magnets
  $\mathcal{P}$ described by the angular divergence θ_r

$$f(\theta_r) = |\vec{\mathcal{P}}|_{\mathrm{max}} \cdot \cos\left((1+a\gamma)\cdot\theta_r\right)$$

Spin Tracking

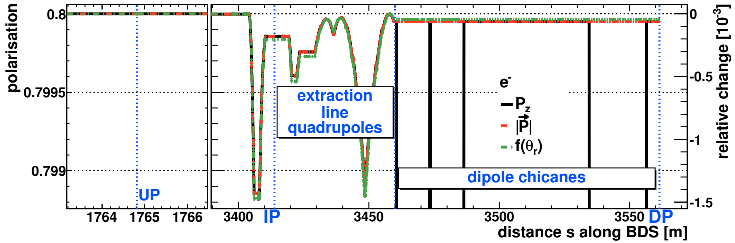

Further causes of longitudinal beam polarization change:

- *Bremsstrahlung:*
  Deceleration by passing through matter $\longrightarrow$ negligible for colliders
- *Beamstrahlung:*
  Deflection by the em-field of the oncoming bunch during collision
- *Synchrotron radiation:*
  Deflection by the em-field of accelerator magnets

Systematic Polarization Uncertainty

contribution	uncertainty $[10^{-3}]$
Beam and polarization alignment at polarimeters and IP ($\Delta\vartheta_{\text{bunch}} = 50\,\mu$rad, $\Delta\vartheta_{\text{pol}} = 25$ mrad)	0.72
Variation in beam parameters (10 % in the emittances)	0.03
Bunch rotation to compensate the beam crossing angle	< 0.01
Longitudinal precession in detector magnets	0.01
Emission of synchrotron radiation	0.005
Misalignments (10 μ) without collision effects	0.43
Total (quadratic sum)	0.85
Collision effects in absence of misalignments	< 2.2

[Ref.:] Thesis Moritz Beckmann (http://bib-pubdb1.desy.de/record/155874)

χ^2-Minimization

- **Defining χ^2 function:**

$$\chi^2 := \sum_{\text{process}} \sum_{\pm\pm} \frac{\left(\sigma_{\text{data}} - \sigma_{\text{theory}}\left(P^-_{e-},\ P^+_{e-},\ P^-_{e+},\ P^+_{e+}\right)\right)^2}{\Delta\sigma^2}$$

- **Variating** $\left(P^-_{e-},\ P^+_{e-},\ P^-_{e+},\ P^+_{e+}\right) \longrightarrow$ **Minimizes** χ^2
- **Toy measurement:**
  - Signal expectation value:
    $\langle D\rangle = \sigma_{\text{theory}} \cdot \varepsilon \cdot \mathcal{L} + \mathfrak{B}$
  - One toy experiment:
    Random Poisson number around each $\langle D\rangle$
  - Determine $P^{\pm}_{e\pm}$ by minimizing χ^2
  - Simplified case for illustration:
    - $\mathfrak{B} = 0$ and $\varepsilon = 1$
    - Statistical uncertainties only
    - Using 10^5 toy measruements

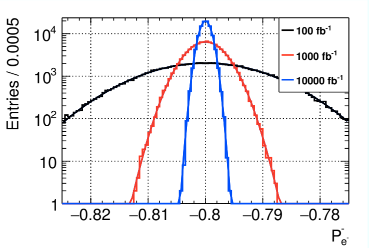

Systematic Uncertainties and their Correlations

- **Systematic Uncertainties are influenced by**
  - Detector calibration and alignment
  - Machine performance
  - ...

⇒ **Time dependent uncertainties**

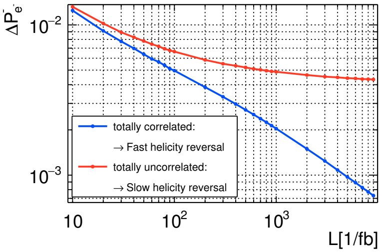

- **Data set are taken one at a time:**
  - Slow frequency of helicity reversals: $\mathcal{O}$ (weeks to months)
  - Data sets are independent
  - → Completely uncorrelated
  - ✘ Lead to saturation at systematic precision

- **Data sets taken concurrently:**
  - Fast frequency of helicity reversals: $\mathcal{O}$ (train-by-train)
  - → Faster than changes in calibration/alignment
  - → Generate correlations
  - ✓ Lead to cancellation of systematic uncertainties

Testing for a Non-Perfect Helicity Reversal

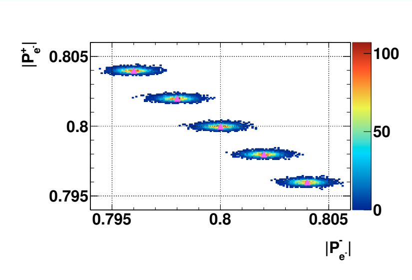

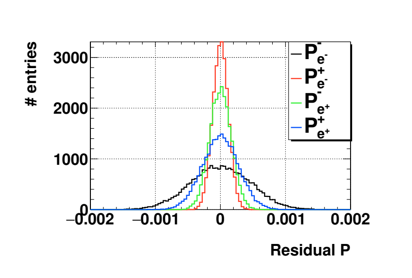

- **Variation in the absolute polarization**
  - Toy Measurement for 5 different polarization discrepancies for both beams
  - Nominal initial polarizations: $|P_{e-}| = 80\%$, $|P_{e+}| = 30\%$
  - Statistical uncertainties only
- **χ^2-Fit:**
  - Correct determination of the 4 polarization values
  - No noticeable impact on polarization precision using total cross sections

✓ **Can compensate for a non-perfect helicity reversal**

Theoretical Limit of the Statistical Precision

Consider most relevant processes:

Process	Channel
single $W^{\pm}$	$e\nu l\nu,\ e\nu q\bar{q}$
WW	$q\bar{q}q\bar{q},\ q\bar{q}l\nu,\ l\nu l\nu$
ZZ	$q\bar{q}q\bar{q},\ q\bar{q}ll,\ llll$
$ZZWW$Mix	$q\bar{q}q\bar{q},\ l\nu l\nu$
Z	$q\bar{q},\ ll$

- Same processes as for physics analysis (DBD)
- Tree-level cross sections + ISR
- Any combination of processes can be used
- Further process can easily added

Consider best case scenario using σ_{tot}:

- Assumption of a perfect 4π detector
- No background
- No systematic uncertainties
- Using all considered processes

Statistical precision H-20: $\Delta P/P\,[\%]$

E	**500**	**350**	**250**	**500**	**250**
$\mathcal{L}$	**500**	**200**	**500**	**3500**	**1500**
$P^-_{e^-}$	0.2	0.3	0.1	0.08	0.09
$P^+_{e^-}$	0.05	0.06	0.03	0.02	0.02
$P^-_{e^+}$	0.1	0.1	0.06	0.04	0.04
$P^+_{e^+}$	0.2	0.3	0.1	0.08	0.08

Generation of Correlated Uncertainties: Fast Helicity Reversal

Generation of Correlated Uncertainties

⇒ Change between data sets $(\sigma_{-+},\ \sigma_{+-},\ \sigma_{--},\ \sigma_{++})$ faster than change in detector and accelerator calibration

⇒ Change between data sets during normal run without additional breaks

ILC Bunch Structure

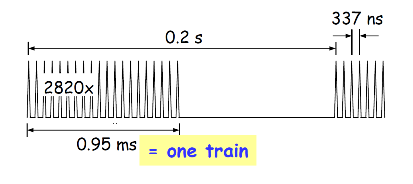

Two possible frequency:

- bunch-by-bunch:
  switch between tow bunches
- train-by-train:
  switch between two trains

- Technical feasibility much easier for train-by-train
- Switch train-by-train should be sufficient for polarization precision

⇒ Precise correlation coefficient still to do

Consideration of the Addition Information from the Angular Distribution

- Total cross section
  - Rely on theoretical calculation
  - ⇒ Susceptible to BSM effects
- Differential cross section
  - Additional usage of the angular information
  - ⇒ Increase of the robustness against BSM effects
- Starting with Single W Process
  - Angular distribution has a large dependence on the chirality
  - Separated in W^+ and W^- production
  - ⇒ Sensitive to individual beam polarization
    - W^+: only sensitive to P_{e^+}
    - W^-: only sensitive to P_{e^-}
- Further processes can easily be included

$$e^- e^+ \longrightarrow W^+ e^- \bar{\nu}_e$$

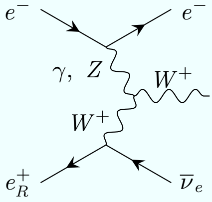

$$e^- e^+ \longrightarrow W^- e^+ \nu_e$$

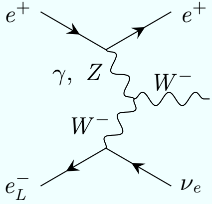

Single $W^{\pm}$: Polar Production Angle Distribution

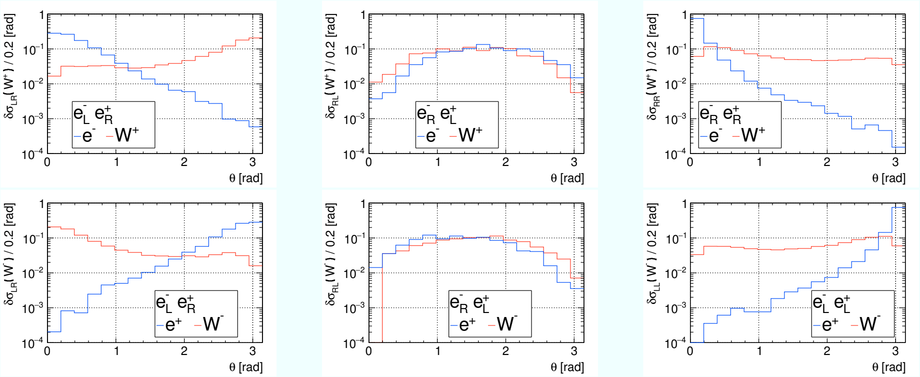

- Single differential cross section: $\partial\sigma/\partial\theta$
  - Two independent angles: $\theta_e,\ \theta_W$
  - For now start with $\theta_e \rightarrow e^{\pm}$ also needed for separation between $W^{\pm}$
- $\partial\sigma/\partial\theta$ will be calculated via $\Delta\sigma_i/\Delta\theta_i$ ("cross section for the i-th bin in θ")

Usage of the Differential Polarized Cross Section

- Total cross section
  - Rely on theoretical calculation
  - ⇒ Susceptible to BSM effects
- Differential cross section
  - Additional usage of the angular information
  - ⇒ Increase of the robustness against BSM effects

e.g.: $e^+e^- \rightarrow W^+W^- \rightarrow q\bar{q}l\nu$

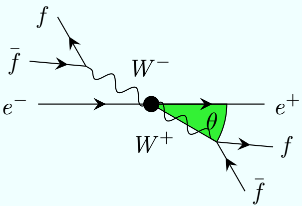

Bin-wise cross section calculation:

$$\overbrace{\partial\sigma/\partial\theta}^{\text{differential cross section}} \longrightarrow \overbrace{\delta_i\sigma_{\text{data}}}^{\text{cross section of the } i\text{-th bin}} := \delta_i N/\mathcal{L}$$

$$\longrightarrow \quad \delta_i\sigma_{LR} := f_{LR}(\theta_i)\cdot\sigma_{LR}$$

Analog: $RL,\ LL,\ RR$

- $\delta_i N$: events of i-th bin
- $f(\theta_i)$: fraction of the total cross section

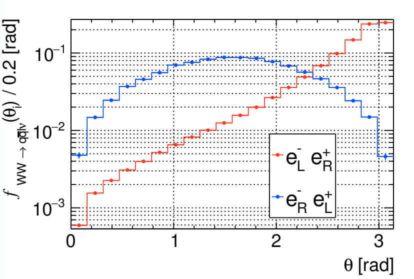

Defining Differential Cross Sections

Measured cross section:

$$\overbrace{\frac{\partial\sigma}{\partial\theta}}^{\text{differential cross section}} \longrightarrow \overbrace{\delta_i\sigma_{\text{data}}}^{\text{cross section per } i\text{th bin}} := \frac{\delta_i D - \delta_i \mathfrak{B}}{\delta_i\varepsilon \cdot \mathcal{L}}$$

$\delta_i D$	Number of signal events	of the ith bin
$\delta_i \mathfrak{B}$	Number of expected background events	of the ith bin
$\delta_i \varepsilon$	Selection efficiency	of the ith bin
$\mathcal{L}$	Integrated luminosity	

Theoretical cross section:

$$\begin{aligned}\delta_i\sigma_{\pm\pm} = & \frac{\left(1\pm\left|P_{e-}^{\pm}\right|\right)}{2}\frac{\left(1\pm\left|P_{e+}^{\pm}\right|\right)}{2}\delta_i\sigma_{RR} + \frac{\left(1\mp\left|P_{e-}^{\pm}\right|\right)}{2}\frac{\left(1\mp\left|P_{e+}^{\pm}\right|\right)}{2}\delta_i\sigma_{LL} \\ + & \frac{\left(1\pm\left|P_{e-}^{\pm}\right|\right)}{2}\frac{\left(1\mp\left|P_{e+}^{\pm}\right|\right)}{2}\delta_i\sigma_{RL} + \frac{\left(1\mp\left|P_{e-}^{\pm}\right|\right)}{2}\frac{\left(1\pm\left|P_{e+}^{\pm}\right|\right)}{2}\delta_i\sigma_{LR}\end{aligned}$$

$$\delta_i\sigma_{\text{theory}} := f\left(\theta_i\right)\cdot\sigma_{\text{theory}}$$

$f\left(\theta_i\right)$ is directly obtained from the angular distributions

Implementing Differential Cross Sections in the χ^2 Minimization

Replacing: $\sigma \longrightarrow \delta_k \sigma$ + Sum over all bins

$$\chi^2 = \sum_{\text{process}} \sum_{\theta_k} \left(\delta_k \vec{\sigma}_{\text{data}} - \delta_k \vec{\sigma}_{\text{theory}}\right)^T \left(\delta_k \Xi\right)^{-1} \left(\delta_k \vec{\sigma}_{\text{data}} - \delta_k \vec{\sigma}_{\text{theory}}\right)$$

$$\delta_k \vec{\sigma} := \begin{pmatrix} \delta_k \sigma_{-+} & \delta_k \sigma_{+-} & \delta_k \sigma_{--} & \delta_k \sigma_{++} \end{pmatrix}^T$$

$$\delta_k \Xi := \delta_k \Xi_N + \delta_k \Xi_{\mathfrak{B}} + \delta_k \Xi_{\varepsilon} + \delta_k \Xi_{\mathcal{L}};$$

$$\left(\delta_k \Xi_{\varepsilon}\right)_{ij} = \text{corr}\left(\vec{\sigma}_i^{\varepsilon},\ \vec{\sigma}_j^{\varepsilon}\right) \frac{\partial\left(\delta_k \vec{\sigma}_i\right)}{\partial\left(\delta_k \varepsilon_i\right)} \frac{\partial\left(\delta_k \vec{\sigma}_j\right)}{\partial\left(\delta_k \varepsilon_j\right)} \Delta\left(\delta_k \varepsilon_i\right) \Delta\left(\delta_k \varepsilon_j\right)$$

Remarks:

- Due to correlations, the binning in θ has to be equal for all cross sections
- It can differ between processes and decay-channels
- Range and number of bins of θ can be changed externally for each process

First Toy Measurements: Preliminary Results

Single $W^{\pm}$ only

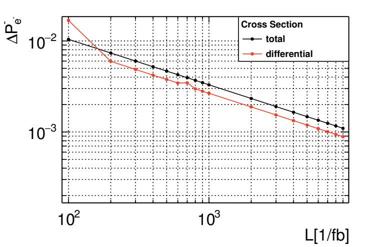

Using the following configuration:

- Using 16 equal bins in a θ range of $[0, \pi]$
- Signal determination bin-by-bin: $\langle \delta_k D \rangle = \delta_k \sigma_{\text{theory}} \cdot \delta_k \varepsilon \cdot \mathcal{L} + \delta_k \mathfrak{B}$
- For the start: Statistical error only + no background
- Using H-20 integrated luminosity sharing due to energy

- Differential cross section have a lower statistic uncertainty:
  - Expectation of $\delta_k D$ can be for some bins $\mathcal{O}(1)$
  - Some zero diagonal entries of the covariance matrix $\rightarrow$ not invertible
  - $\Rightarrow$ Dropping χ^2-terms with $\delta_k D = 0$
- Further steps:
  - Optimizing the θ range and binning
  - Including further processes